New approach to the mixed-valence problem

Piers Coleman
Joseph Henry Laboratories, Department of Physics, Princeton University, Jadwin Hall, P.O. Box 708, Princeton, New Jersey 08540
(Received 29 August 1983)

A new formulation of the mixed-valence problem is presented in which the singlet valence state of a rare-earth ion is represented by a zero-energy boson and the spinning state by a spin-j fermion. This representation avoids the need to use Hubbard operators with awkward algebras and avails itself of standard techniques for dealing with interacting quantum systems. In particular, a Feynman-diagram expansion for the thermodynamic variables and spectral functions can be developed. The advantages of the approach are illustrated for the mixed-valence impurity problem. Vertex corrections are found to be $O(1/N^2)$, where N is the degeneracy of the rare-earth ion, allowing a self-consistent calculation of the f-electron spectral function to order $O(1/N^2)$ that is valid in both the mixed-valence and Kondo regimes. The extension to the lattice is outlined and some preliminary results reported.

I. INTRODUCTION

In recent years the mixed-valence problem has aroused considerable interest among theoretical condensed-matter physicists.[1,2] The great allure of the mixed-valence problem lies in the deceptive simplicity of the standard mixed-valence model. In a mixed-valence crystal there is a lattice of rare-earth ions which can exist in two valence states, one of which is typically a singlet, the other a $2j+1$ $(=N)$ -fold-degenerate state of spin j. There is an extended band of free electrons which hybridizes weakly with the rare-earth f states causing the valence to fluctuate by changes in the f-level occupation

$$f_n \rightleftarrows f_{n-1} + e^- .$$

The weakness of the hybridization makes it very attractive to try to consider it as a perturbation. The crux of the mixed-valence problem is that this is not a trivial task.

The simplest mixed-valence system, where $n=1$, illustrates the difficulties. Here the valence fluctuations are between an $|f^0; j=0\rangle$ and a $|f^1; j,m\rangle$ state. The standard model Hamiltonian describing the system is the infinite-U Anderson model.[3,4] which can be written

$$H = H_{\text{band}} + \sum_i H_f^i + \sum_i H_{\text{mix}}^i , \tag{1}$$

where

$$H_{\text{band}} = \sum_{\vec{k},\sigma} E(k) c^\dagger_{\vec{k}\sigma} c_{\vec{k}\sigma} \tag{2}$$

describes the free-electron band, while

$$H_f^i = \sum_{m=-j}^{m=j} E_f f_m^{i\dagger} f_m^i \tag{3}$$

describes the f state at each lattice site i, and

$$H_{\text{mix}}^i = \sum_{\vec{k},m=-j}^{m=j} [V(k) c^{i\dagger}_{\vec{k}m} P_0 f_m^i + \text{H.c.}] \tag{4}$$

is the term which mixes the two valence states at site i. The operator P_0 projects out states with no f electrons at site i so that charge fluctuations only occur between two valence states. The operator $c^{i\dagger}_{km}$ creates a band electron of energy $E(k)$ in the angular momentum scattering channel $|jm\rangle$ at site i. The full Hamiltonian H is taken implicitly to act in the subspace of states S with either zero or one f electrons at each site.

The great difficulty in treating H_{mix} as a perturbation arises because the Hubbard operators, $X^i_{0m} = P_0 f^i_m$ and $X^i_{m0} = f^{i\dagger}_m P_0$, do not obey standard fermion commutation rules.[4,5] This is of course a consequence of the strong interaction between f electrons at one site. It means that there is no Wicks theorem for the Hubbard operators and precludes the application of conventional quantum-field-theory techniques.

Keiter and Kimball[5] recognized that the awkward commutation rules of the Hubbard operators restricted one to a time-ordered perturbation theory, which they developed for the case of the mixed-valence impurity. Subsequent treatments of the mixed-valence problem, both for the impurity[6–8] and the lattice[9] have been based on their approach. The great disadvantage of a time-ordered perturbation theory is that it is awkward to evaluate the diagrams and very difficult to carry out the resummations of the diagrams. Recently, serious doubts have been raised concerning the validity of resummations that have been used to extend the Keiter-Kimball technique to the lattice,[10] further emphasizing the problems inherent in this approach.

In this paper an alternative approach is presented which avoids these difficulties by using operators that obey standard fermion or boson algebras. The basic idea is to replace the awkward Hubbard operators by a product of a boson and fermion operator,

$$X^i_{0m} \rightarrow b^{i\dagger} f^i_m , \tag{5}$$

$$X^i_{m0} \rightarrow f^{i\dagger}_m b^i . \tag{6}$$

The mathematical motivation behind this replacement is that these operators can be treated using standard field

theory. The physical interpretation of this replacement is that the spinless valence state f^0 is now represented by a boson that is created when an f electron hops out of the rare-earth ion and destroyed when a band electron hops into the rare-earth ion.

The essence of this approach was invented by Barnes,[11] who employed two bosons to represent the singlet states of the spin-$\frac{1}{2}$ Anderson model. In this new application to the mixed-valence problem only one boson is required per rare-earth ion which proves to be a useful simplification.

To illustrate the approach the mixed-valence impurity will be considered first, and the generalization to the lattice is made later by introducing appropriate indices. The new Hamiltonian corresponding to the above approach is

$$H' = H_{\rm band} + H_f + H_{\rm mix} + \epsilon b^\dagger b \tag{7}$$

Here $H_{\rm band}$ and H_f are the same as before (there is no site index in the impurity problem) while the transformations (5) and (6) have been made to produce the new mixing Hamiltonian

$$H_{\rm mix} = \sum_{\vec{k},m} \{ V(k) c^\dagger_{km} (b^\dagger f_m) + [V(k)]^* (f^\dagger_m b) c_{km} \} . \tag{8}$$

With this new Hamiltonian, the number operator

$$Q = b^\dagger b + n_f \tag{9}$$

commutes with H' so the total number of f electrons plus bosons is conserved. $H_{\rm mix}$ converts bosons into f electrons and vice versa, conserving the charge Q. This means that each of the subspaces F_Q with definite Q are disjoint. The interesting subspace is F_1 where $H_{\rm mix}$ induces transitions between the singly occupied boson state b^1 and the $2j+1$ $(=N)$ -fold-degenerate fermion state f^1_m:

$$f^1 \rightleftarrows b^1 + e^- . \tag{10}$$

Clearly, within this subspace the boson state can be identified with the singlet state of the rare-earth ion:

$$|f^0\rangle \equiv b^\dagger |0\rangle , \quad |f^1; j,m\rangle \equiv f^\dagger_m |0\rangle . \tag{11}$$

With this identification, the matrix elements of $H_{\rm mix}$ within F_1 are identical to those of $H_{\rm mix}$ in S,

$$\{H_{\rm mix}: \ \psi \in S\} \equiv \{H_{\rm mix}: \ \psi \in F_1\} . \tag{12}$$

Finally, since $H_{\rm band}$ and H_f are identical in both subspaces, setting the boson energy ϵ to zero, it is seen that H and H' are equivalent in these subspaces,

$$\{H'\}_{\psi \in F_1} \equiv \{H\}_{\psi \in S} . \tag{13}$$

So the valence fluctuation $f^1 \rightleftarrows f^0 + e^-$ can be represented by a resonance between a zero-energy boson and a spin-j fermion in the subspace where $Q = n_b + n_f = 1$. Since the subspaces are disjoint, it is an easy task to project out this subspace. The extension to the lattice is made by introducing a zero-energy boson for each site, with the appropriate interaction $H^i_{\rm mix}$ at the ith site. Hence,

$$H^i_{\rm mix} = \sum_{\vec{k},m} [V(k) c^{i\dagger}_{km} b^{i\dagger} f^{i\dagger}_m + {\rm H.c.}] \tag{14}$$

The appropriate subspace for the mixed-valence lattice is that in which $Q_i = 1$ at each site. The great advantage of this new technique is that a broad range of powerful quantum-field-theory techniques can now be brought to bear on the mixed-valence problem because the operators all obey standard algebras.

II. APPLICATION OF THE BOSON TECHNIQUE

The application of this new approach is illustrated using the mixed-valence impurity, and full extension to the lattice will only be outlined, awaiting completion of further work. In this illustration the emphasis will be placed on the development of a diagrammatic expansion, in keeping with the original motivation. However, it should be borne in mind that path-integral techniques can be applied to this reformulation, which provides the interesting new possibility of integrating out the fermionic degrees of freedom, and then carrying out a saddle-point approximation for the integration over the bosonic degrees of freedom.

The development of a diagrammatic expansion for the partition function of H' closely parallels that used for the Kondo lattice problem.[12] In order to project out the subspace F_1, a chemical potential $-\lambda$ is associated with the charge Q and the grand-canonical partition function $Z_G(1)$ calculated for $H' + \lambda Q$. Because Q is conserved, $Z_G(\lambda)$ can be expressed as a sum of the canonical partition functions $Z_c(Q)$ for each subspace F_Q,

$$Z_G(\lambda) = {\rm Tr}(e^{-\beta(H' + \lambda Q)}) = \sum_{Q=0}^{\infty} Z_c(Q) e^{-\beta \lambda Q} . \tag{15}$$

The mixed-valence partition function is $Z_c(1)$, and it may be projected out by differentiating Z_G with respect to the fugacity $\zeta = e^{-\beta\lambda}$,

$$Z_{\rm MV} = Z_c(1) = \lim_{\lambda \to \infty} \frac{\partial}{\partial \zeta} [Z_G(\lambda)] . \tag{16}$$

By writing $Z_G(\lambda) = \exp[-\beta F(\lambda)]$, where $F(\lambda)$ is the free energy, and identifying $\partial F / \partial \lambda = \langle Q \rangle_\zeta$, the expectation value of Q in the grand-canonical ensemble (GCE), leads to

$$Z_{\rm MV} = (\lim_{\lambda \to \infty} \zeta^{-1} \langle Q \rangle_\lambda) Z_{\rm band} , \tag{17}$$

where the $\zeta \to 0$ limit of $Z_G(\lambda)$ has been identified as the partition function of the free-electron band $Z_{\rm band}$. In a similar manner the expectation value of any operator O in the canonical ensemble of F_1 can be calculated using the GCE expectation value and taking the limit of large λ. Consider $\langle OQ \rangle_\lambda$,

$$\langle OQ \rangle_\lambda = \sum_{Q=0}^{\infty} ({\rm Tr} O e^{-\beta H'})_{F_Q} Q e^{-\beta \lambda Q} / Z_G(\lambda) . \tag{18}$$

Thus

$$\langle O \rangle_{F_1} = ({\rm Tr} O e^{-\beta H'})_{F_1} / Z_c(1) = \lim_{\lambda \to \infty} (\langle OQ \rangle_\lambda / \langle Q \rangle_\lambda) . \tag{19}$$

In general the operators of interest will have zero expectation value in the F_0 subspace and in the large-λ limit $\langle OQ \rangle_\lambda \to \langle O \rangle_\lambda$, enabling Q to be left out of the numerator in (19),

$$\langle O\rangle_{F_1}=\lim_{\lambda\to\infty}(\langle O\rangle_\lambda/\langle Q\rangle_\lambda)\,. \tag{20}$$

Equations (20) and (17) are the essential relationships between the GCE and the canonical ensemble with $Q=1$, enabling the properties of the F_1 subspace to be projected from the properties of the GCE.

$H_{\rm mix}$ can be treated as a perturbation about $H_0=H_f+H_{\rm band}$, and the grand partition function can be expanded as the path-ordered exponential of $H_{\rm mix}$,

$$H_{\rm mix}(\tau)=e^{\tau H_0}H_{\rm mix}e^{-\tau H_0}\,, \tag{21}$$

$$\frac{Z_G(\lambda)}{Z_G(H_0,\lambda)}=\left\langle T\exp\left[-\int_0^\beta H_{\rm mix}(\tau)d\tau\right]\right\rangle_{H_0}\,. \tag{22}$$

Here $\langle\ \rangle_{H_0}$ denotes the expectation value in the noninteracting GCE.

The perturbation expansion of the path-ordered exponential is a standard summation of closed-loop connected and disconnected Feynman diagrams containing the bare propagators

$$G^0_{fm}(\tau)=\langle Tf_m(\tau)f^\dagger_m(0)\rangle_{H_0}$$
$$=-k_BT\sum_{\omega_n}e^{-i\omega_n\tau}/(i\omega_n-\lambda-E_f)\,, \tag{23}$$

$$D^0(\tau)=\langle Tb(\tau)b^\dagger(0)\rangle_{H_0}$$
$$=-k_BT\sum_{\nu_n}e^{-i\nu_n\tau}/(i\nu_n-\lambda)\,, \tag{24}$$

$$G_{\vec{k}m}(\tau)=\langle c_{\vec{k}m}(\tau)c_{\vec{k}m}(0)\rangle_{H_0}$$
$$=-k_BT\sum_{\omega_n}e^{-i\omega_n\tau}/[i\omega_n-E(k)]\,, \tag{25}$$

linked together by the interaction vertices generated by $H_{\rm mix}$. The associated Feynman diagrams for these propagators are illustrated in Fig. 1. A directed arrow is used to show the flow of charge Q along boson lines.

As usual, the path-ordered exponential can be expressed as the exponential of the change in free energy ΔF, and ΔF is given by a sum of connected closed-loop diagrams as shown in Fig. 2.[13] In each connected diagram there are

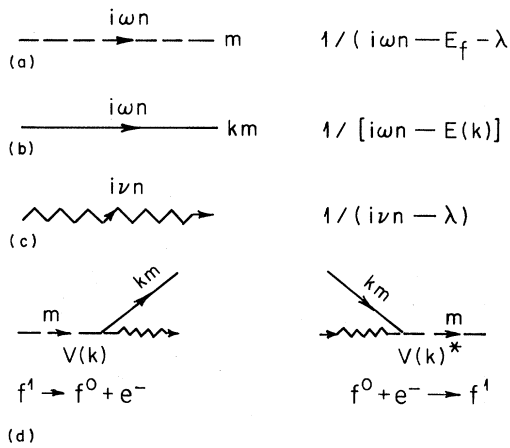

FIG. 1. Notation used in Feynman diagrams: (a) f-electron propagator, (b) band-electron propagator, and (c) boson propagator with directed line showing flow of charge Q.

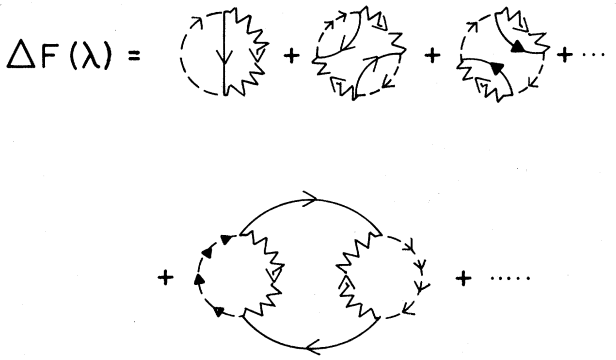

FIG. 2. Closed-loop diagrams contributing to the expansion of the free energy.

a certain number of closed loops around which charge flows (Fig. 3). For each of these closed loops there is a factor of the fugacity ζ so that when the $\lambda\to\infty$ limit is taken, the diagrams with a large number of loops vanish relative to the $Q=1$ diagrams.

There are two valuable results of this formalism. Firstly, a closed expression for $Z_{\rm MV}$ can be written in terms of the full boson and fermion propagators. Because of the chemical potential $-\lambda$, the spectral functions of the f electron are centered around $\omega=\lambda$, thus defining the spectral densities by

$$A_{fm}(\omega)=\pi^{-1}{\rm Im}G_{fm}(\omega+\lambda-i\delta)\,, \tag{26}$$

$$B(\nu)=\pi^{-1}{\rm Im}D(\nu+\lambda-i\delta)\,, \tag{27}$$

where G_{fm} and D are the full propagators in the interacting GCE; $\langle Q\rangle_\zeta$ is then given by

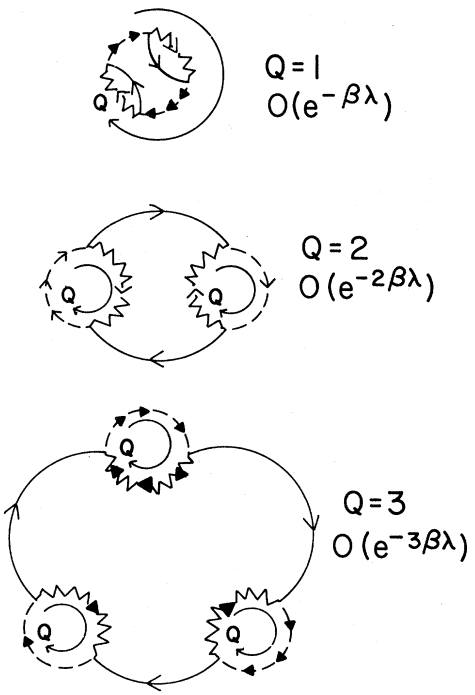

FIG. 3. Fugacity dependence of connected diagrams containing different number of loops carrying charge Q.

$$\langle Q\rangle_\zeta = \int_{-\infty}^{\infty} d\omega \left[\sum_m A_{fm}(\omega) f(\omega+\lambda) + B(\omega) n(\omega+\lambda) \right] , \tag{28}$$

where $f(\omega)=[\exp(\beta\omega)+1]^{-1}$ and $n(\omega)=[\exp(b\omega)-1]^{-1}$ are the Fermi and Bose functions. By substituting this expression into (27), the partition function for the mixed-valence impurity is thus

$$Z_{\rm MV}(\beta) = \lim_{\lambda\to\infty} \int_{-\infty}^{\infty} d\omega \left[\sum_m A_{fm}(\omega) + B(\omega) \right] e^{-\beta\omega} . \tag{29}$$

The $\lambda\to\infty$ limits of A_{fm} and B are well defined because the displacement of the chemical potential has been subtracted out. However large λ becomes, the band electrons will still produce a resonance between the boson and fermion state because the separation of their bare energies is always E_f. Thus if the propagators are expanded in terms of their self-energies (Fig. 4)

$$\begin{aligned} G_{fm}(\omega) &= [\omega - E_{fm} - \Sigma_{fm}(\omega) - \lambda]^{-1} , \\ D(\nu) &= [\nu - \Pi(\nu) - \lambda]^{-1} , \end{aligned} \tag{30}$$

it may be deduced that the self-energies contain an imaginary part, giving rise to a width in the spectral functions. The peaks of the spectral functions will occur at energies E_f^* and E_b^* given by

$$\begin{aligned} E_{fm}^* &= E_{fm}^* + \mathrm{Re}[\Sigma_{fm}(E_{fm}^*+\lambda)] , \\ E_b^* &= \mathrm{Re}[\Pi(E_b^*+\lambda)] . \end{aligned} \tag{31}$$

These expressions are the analogs to the Brillouin-Wigner expressions derived by Keiter and Kimball.[5] Provided the temperature exceeds the widths of the spectral functions at the lowest-energy poles, the spectral functions can then be treated as δ functions in the integral (29), reproducing the well-known Keiter-Kimball expression for the partition function,

$$Z_{\rm MV}(\beta) = e^{-\beta E_b^*} + \sum_m e^{-\beta E_{fm}^*} . \tag{32}$$

Below a critical temperature characterizing the slow spin and charge fluctuations of the system, the Keiter-Kimball result becomes an approximation because the widths of the spectral functions can no longer be ignored. The regularization procedure used in the time-ordered perturbation theory explicitly ignores these widths by forcing the self-energies to be real. This is why the time-ordered perturbation theory can not extend to the Kondo regime.

The other useful application of the boson technique is to calculate the spectral function of the real f electron. In terms of the Hubbard operators, the propagator for the real f electron is given by

$$\mathcal{G}_m(\tau) = \langle T[X_{0m}(\tau) X_{0m}(0)] \rangle_H , \tag{33}$$

which in terms of the boson approach becomes

$$\mathcal{G}_m(\tau) = \langle T[b^\dagger(\tau) f_m(\tau) f_m^\dagger(0) b(0)] \rangle_{F_1} . \tag{34}$$

By using (22), this becomes

$$\mathcal{G}_m(\tau) = \lim_{\lambda\to\infty} [\langle T b^\dagger(\tau) f_m(\tau) f_m^\dagger(0) b(0)\rangle_\lambda / \langle Q\rangle_\lambda] . \tag{35}$$

The numerator in this expression is simply the two-particle correlation function $C_m(\tau)$ shown in Fig. 5. $C_m(\tau)$ can be expressed in terms of the full boson and fermion propagators, integrated with a vertex term $\Lambda(\tau_1,\tau_2)$ for the renormalized mixed-valence interaction. Hence,

$$C_m(\tau) = \int_0^\beta d\tau_1 d\tau_2 G_m(\tau_2) D(-\tau_1) \Lambda(\tau-\tau_2, \tau-\tau_1) . \tag{36}$$

Now, in general, calculation of these spectral functions would be thwarted by the difficulty of calculating vertex functions. Vertex functions enter into the expansions of the boson and fermion self-energies as well as the real f spectral function. The problem is solved by recognizing that for typical mixed-valence systems, the degeneracy is large, and in the limit of large degeneracy the vertex corrections are of order $O(1/N^2)$ and can be neglected.

To see this in detail, consider the large-N limit. To produce a well-defined large-N limit the bare interaction vertex must be rescaled according to

$$V(k) = \tilde{V}(k)/\sqrt{N} , \tag{37}$$

where $\tilde{V}(k)$ is kept fixed as N is made large.[14,9] Now in a general diagram of order $1/N^R$, if Λ is the number of vertices and L is the number of closed fermion loops, then

$$R = \Lambda/2 - L \tag{38}$$

because each vertex adds a factor of $1/N$, and each closed fermion loop adds a factor of N due to the summation over N spin states. Now the vertex functions are deter-

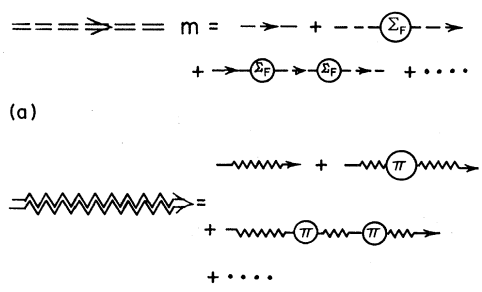

FIG. 4. Expansion of full propagators in terms of self-energies. (a) Fermion propagator, and (b) boson propagator.

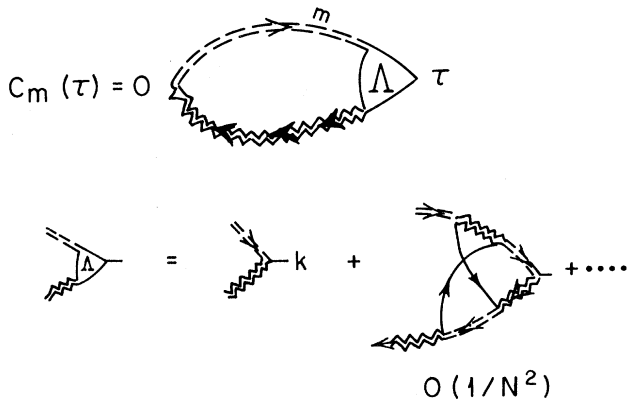

FIG. 5. Diagrammatic expansion of real f-electron Green's function showing the vertex corrections.

mined by the irreducible two-particle Green's functions, and for a general diagram contributing to these functions the number of links between the external lines, $\Lambda/2$ must exceed the number of closed fermion loops by 2 (Fig. 6) or more, so that $\Lambda/2-L\geq 2$ leading to the above result. It is interesting to remark that the general n-particle irreducible Green's function must be of order $O(1/N^n)$ for similar reasons. From general field theory it is known that the n-particle vertices Γ^n determine the functional dependence of the free energy on the fields[15] according to

$$\beta F[f^\dagger,f,b^\dagger b]=\int_0^\beta d\tau d\tau'[f^\dagger(\tau)G^{-1}(\tau-\tau')f(\tau')+b^\dagger(\tau)D^{-1}(\tau-\tau')b(\tau')] + \int_0^\beta d\tau d\tau' d\tau'' d\tau'''[f^\dagger(\tau)f(\tau')\Gamma^2(\tau,\tau',\tau'',\tau''')b^\dagger(\tau''')b(\tau'''')]+\cdots , \tag{39}$$

where the ellipsis includes the higher-order vertices. Here spin subscripts have been left out, and the band-electron degrees of freedom have been integrated away. Thus a rigorous expansion of the free-energy functional to order $O(1/N^2)$ can be obtained by ignoring vertex corrections and higher-order interactions. Formally, the partition function and thermal Green's functions are determined by minimizing the free-energy functional, so this is the best $1/N$ expansion that can be carried out. This approximation is subtler than merely taking the highest-order diagrams in the expansion of the propagators. These arguments are independent of whether one is the "Kondo" or "mixed-valence" regimes.

This result can be exploited to produce expressions for the boson, fermion, and real f-electron propagators that are accurate to $O(1/N^2)$. The self-consistent diagrams for the expansion to this order are shown in Fig. 7. The dominant $O(1)$ effect is the renormalization of the boson self-energy $\Pi(\nu)$. The fermion self-energies are of leading order $O(1/N)$. This is consistent with the results of Ramakrishnan,[8] who showed that large degeneracy results in a lowering of the empty-state energy E_0 that is N times larger than the lowering of the energy E_f of the full state.

Carrying out the frequency sums in these diagrams is a straightforward task, and taking the large-λ limit, the self-consistent equations for the boson and fermion Green's functions are (see Appendix A)

$$\Sigma_{fm}(\omega)=N^{-1}\sum_k |\tilde{V}(k)|^2 D(\omega+E(k))f(E(k)) ,$$
$$\Pi(\omega)=\sum_{\vec{k},m} |\tilde{V}(\vec{k})|^2 G_{fm}(\omega+E(k))f(E(k)) . \tag{40}$$

In this expression the large-λ limit has been taken and frequencies are measured relative to the chemical potential $-\lambda$. The real f-electron spectral function $\rho_m(\omega)$ is given by the convolution of A_{fm} with B according to

$$\rho_m(\omega)=\int_{-\infty}^{\infty} d\nu[A_{fm}(\omega+\nu)B(\nu)] \times[e^{-\beta(\omega+\nu)}+e^{-\beta\nu}]/Z_{\mathrm{MV}}(\beta) . \tag{41}$$

To date the author has not obtained analytic solutions to these equations, though their qualitative features are deduced from simple arguments and numerical solutions are readily obtained by iteration. An alternative approach would be to numerically integrate away the band electrons in Eqs. (40) by progressively reducing the bandwidth. Such an approach was not used here, but it is worth noting that it would correspond to a dynamic version of Haldane scaling.[16]

By considering the spectral decomposition of A_{fm} and B (see Appendix B) the general form of the spectral functions can be shown to be

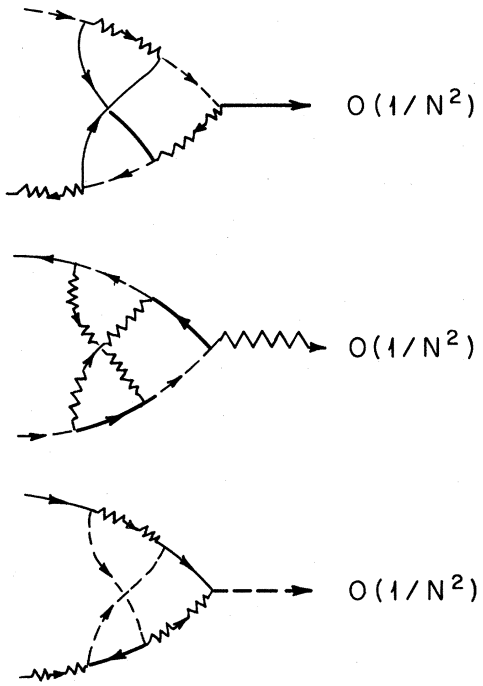

FIG. 6. Showing how vertex corrections are of order $O(1/N^2)$.

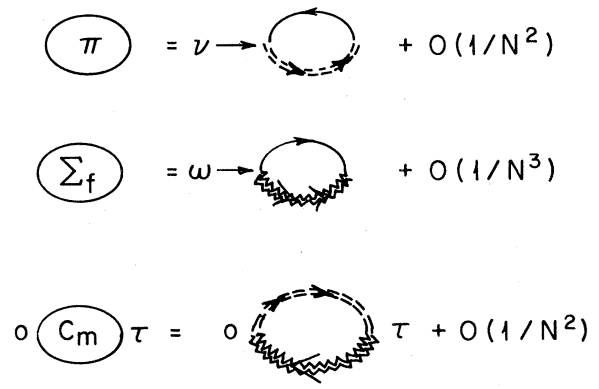

FIG. 7. Diagrams for the self-consistent expansion of propagators and self-energies to order $O(1/N^2)$.

$$A_{fm}(\omega)=\Theta(\omega-E_0)A^+_{fm}(\omega)+\Theta(E_0-\omega)Z_{\rm MV}(\beta)e^{\beta\omega}a_{fm}(\omega)\,,$$
$$B(\nu)=\Theta(\nu-E_0)B^+(\omega)+\Theta(E_0-\nu)Z_{\rm MV}(\beta)e^{\beta\nu}b(\nu)\,, \tag{42}$$

where the functions A^+, B^+, and a,b all have well-defined and finite zero-temperature limits. E_0 is the ground-state energy of the F_1 subspace measured relative to the energy of the unperturbed electron sea. At low temperatures $Z_{\rm MV}\sim e^{-\beta E_0}$, and so the second terms in these expressions form exponential tails which vanish at absolute zero. At absolute zero $A^+(\omega)$ and $B^+(\omega)$ are the energy spectra of the states formed by adding a single boson or f electron to the unperturbed electron sea. These spectra necessarily contain x-ray singularities at their threshold energies[17,18] because changing the number of bosons or f electrons means that the charge Q is changed, and so the band electrons experience a new scattering potential, resulting in a power-law relaxation of the electron sea as an infinite cascade of electron-hole pairs are produced. The fully relaxed new ground state has no overlap with the initial state. Consider the addition of a boson to the unperturbed electron sea to form the state $b^\dagger|0;Q=0\rangle$. Then the propagator for this state will have a power-law dependence on time at long times that is characteristic of infrared catastrophies,

$$\langle 0;Q=0\,|\,T[b(t)b^\dagger(0)]\,|\,0;Q=0\rangle\sim 1/t^\alpha\,, \tag{43}$$

consequently $B(\nu)\sim|\nu-E_0|^{\alpha-1}$. By substituting this into the zero-temperature limit of Eq. (40) and iterating once gives $A_m(\omega)\sim|\omega-E_0|^{-\alpha}$. By iterating twice, α is constrained to $\alpha=1/(1+N)$ and the low-energy forms of $D(\nu)$ and $G_m(\omega)$ are deduced to be

$$D(\nu+i\delta)\sim-[e^{iN\pi/N+1}/(\nu-E_0)^{N/N+1}]\,,$$
$$G_m(\omega+i\delta)\sim[e^{i\pi/N+1}/(\omega-E_0)^{1/N+1}]\,, \tag{44}$$

To accuracy $O(1/N^2)$, $\alpha=1/N$, a result that could have been deduced from Nozieres and De Dominicis' theory,[18] assuming N scattering channels, and each scattering with a phase shift $\delta=\pi/N$ corresponding to the single $Q=1$ bound state. By their formula, $\alpha=\sum\delta^2/\pi^2=1/N$. This may well be an exact result.

By substituting the expressions (42) in the expression (41) the spectrum of the real f state at absolute zero is given by

$$\rho_m(\omega)=\Theta(\omega)\int_{E_0}^{E_0+\omega}A^+_{fm}(\omega+\nu)b(\nu)d\nu$$
$$+\Theta(-\omega)\int_{E_0+\omega}^{E_0}a_{fm}(\omega+\nu)B^+(\nu)d\nu\,. \tag{45}$$

For $\omega\sim0$ the products in these integrals are $\sim1/\nu$, giving a finite and smooth real f spectral function at the Fermi surface. Here the functions $a_{fm}(\nu)$ and $b(\nu)$ act as smoothing functions, and it can be loosely said that the real f spectrum below the Fermi surface has the broadened shape of the boson spectral function (reflected) while the real f spectrum above the Fermi surface has the shape of the f-fermion spectral function $A^+_{fm}(\omega)$. One is forced to conclude that at all times the full f spectrum will possess a two-peaked structure.

Numerical work confirms these arguments and produces two-peaked spectral functions whose shapes may be classified according to the three well-known regimes of the Anderson model deduced from scaling theory:[16,19] (i) the empty impurity limit, (ii) the mixed-valence regime, and (iii) the Kondo regime. Typical spectra for these regimes are shown in Fig. 8. These spectra were calculated for a uniform band centered on the Fermi energy with constant $V(\vec{k})=V$ and density of states ρ. In regime (i) there is a large peak of weight ~1 per spin channel lying above the Fermi level at the empty f-state energy, having width $\Delta=\pi|V|^2\rho$. As the bare f-state energy E_f becomes of order $-O(N\Delta)$, this peak moves down towards the Fermi energy, and begins to cross it when $E_f\sim-N\Delta$. This is the mixed-valence regime (see Fig. 9). As the bare f energy is further reduced the peak above the Fermi energy cannot move below it; it simply narrows into a Kondo resonance of width T_K/N, and its weight reduces as E_f is lowered. At this point the boson spectral function begins to contribute increasingly to the real f spectral function, producing a broad peak of width $\sim N\Delta$ centered at about $\sim E_f$, whose weight grows to $1/N$ per spin channel (i.e., total weight 1) as one enters the Kondo regime.

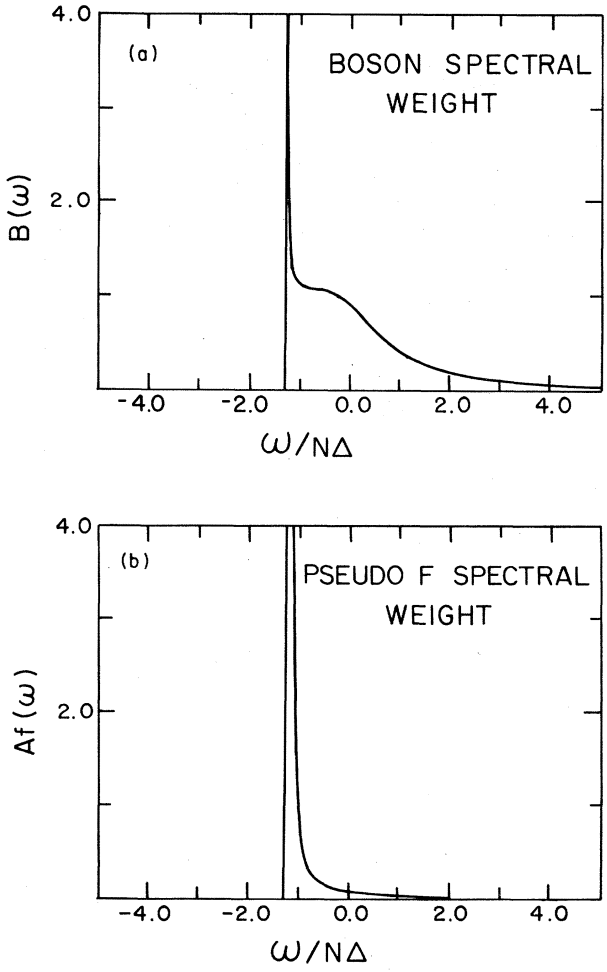

FIG. 8. Typical fermion and boson spectral functions. (a) $B(\nu)$, the boson spectrum, and (b) $A(\omega)$, the fermion spectrum. For these spectra $N=6$, $E_f/N\Delta=-1.1$, and the bandwidth $=10N\Delta$.

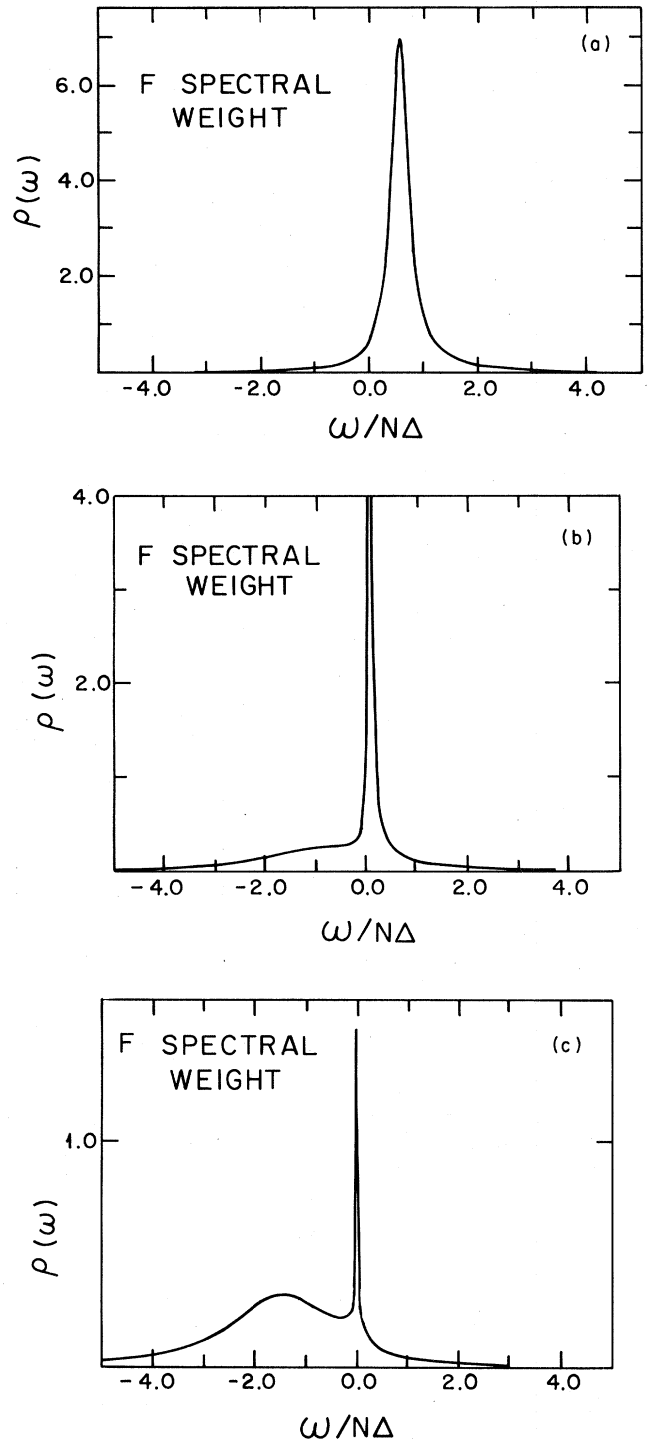

FIG. 9. Real f-state spectrum, $N=6$, bandwidth$=10N\Delta$. (a) $E_f=0$, empty impurity regime; (b) $E_f/N\Delta=-1.1$, mixed-valence regime; (c) $E_f=-2.0N\Delta$, Kondo regime.

III. DISCUSSION: FURTHER DEVELOPMENTS AND THE IMPORTANCE OF INFRARED DIVERGENCES

Before discussing further developments an important issue to be dealt with is the importance of infrared divergences. From the above considerations, it is known that quite rigorously, the overlap of the full mixed-valence impurity ground state $|0;Q=1\rangle$ with the state $b^\dagger|0;Q=0\rangle$ is zero. Translating into the language of the conventional representation of the Anderson Hamiltonian this means that there is absolutely no overlap of the unperturbed Fermi sea $|0\rangle$ with the true mixed-valence impurity ground state $|\Phi_0\rangle$,

$$\langle\Phi_0|0\rangle=0\,. \tag{46}$$

It has been traditional to use variational wave functions as models for the mixed-valence impurity ground state. These variational wave functions have a finite overlap with $|0\rangle$,[1,14] a sign that they do not incorporate these infrared effects.

From the above discussion it is apparent that infrared effects become weak in the large degeneracy limit, as the exponent α vanishes as $O(1/N)$. However, caution must accordingly be applied when interpreting the results of any calculation that ignores these $1/N$ effects, for while they vanish in a system of infinite degeneracy, they are always present in systems with finite degeneracy. The high-energy features of such a calculation are reliable, as are predictions of the ground-state energy and derived quantities such as magnetic susceptibility, for none of these are crucially dependent on infrared effects. It remains unclear how reliable the predictions for the low-energy excitation spectra can be if infrared effects are ignored. One well-known artifact of an "infinite-N" calculation is the presence of a phase transition at finite temperatures,[20,21] which is not present in a finite-N calculation due to infrared effects.

The application of the boson approach to yield a Feynman-diagram expansion for mixed valence is only meant as an illustration of the value of this approach, and further developments are envisaged. One of the great drawbacks of the diagrammatic approach is that it gives a closed expression for the partition function rather than the free energy. This makes it difficult to treat the low-energy thermodynamic properties, and although in principle, the diagrammatic treatment should yield an analytic expression for the Wilson ration $R=\chi/\gamma$ that is accurate to $O(1/N^2)$, the author has not succeeded in deriving it. A path-integral approach may be more appropriate for low-temperature properties, as in the case of the Kondo problem.[20]

However, there is much to be learned from an extension of the diagrammatic treatment to the lattice. This extension is achieved by introducing a conserved charge Q_i for each site and an associated chemical potential $-\lambda_i$. The partition function for the lattice is then given by

$$Z_{\text{lattice}}(\beta)=\lim_{\lambda_i\to\infty}\prod_i\frac{\partial}{\partial\zeta_i}[Z(\lambda_1,\lambda_2,\ldots,\lambda_i)]\,. \tag{47}$$

The partition function for the GCE can be expanded as a sum of closed-loop Feynman diagrams, as in the impurity problem, and the projection operation selects those diagrams with one closed loop for each charge Q_i. As in the analogous Kondo lattice problem[12], this generates a cluster expansion for the partition function,

$$\frac{Z_{\text{lattice}}(\beta)}{Z_{\text{band}}} = \lim_{\lambda_i \to \infty} \left[\alpha^r \left[1 + \sum_i \frac{Z_i}{\alpha \zeta_i} + \sum_{i,j} \frac{(Z_{ij} + Z_i Z_j)}{\alpha^2 \zeta_i \zeta_j} + \cdots \right] \right], \quad (48)$$

where r is the number of sites and the terms $Z_{i,j,..,n}$ are the sums of all closed-loop connected diagrams connecting sites $i, j, \ldots, n$, while α is the partition function of a noninteracting rare-earth ion,

$$\alpha = 1 + \sum_m \exp(-\beta E_{fm}) .$$

Most important of all is the existence of a $1/N$ expansion for the partition function. In the general p-site term,

$$\Lambda/2 \geq L + (p-1) \quad (49)$$

(see Fig. 10). Thus by (38) the general p-site term is of order $O(1/N^{p-1})$. This confirms the conjecture of Ramakrishnan[8] that to all orders in perturbation theory, intersite interactions are smaller by orders of $1/N$, a result already known for the Kondo lattice.[12] It means that the local picture of mixed valence will be a good approximation in the large-N limit.

To produce a consistent expansion of the free energy of the lattice to order $O(1/N^2)$ it will thus be sufficient to consider just one-site and two-site interactions. To this order it is found that two new intersite interactions enter into the problem, both of order $O(1/N)$ (Fig. 11): an interaction between empty states, and a hopping term which will tend to delocalize the f electrons (Fig. 10). Later work will develop these ideas in detail.

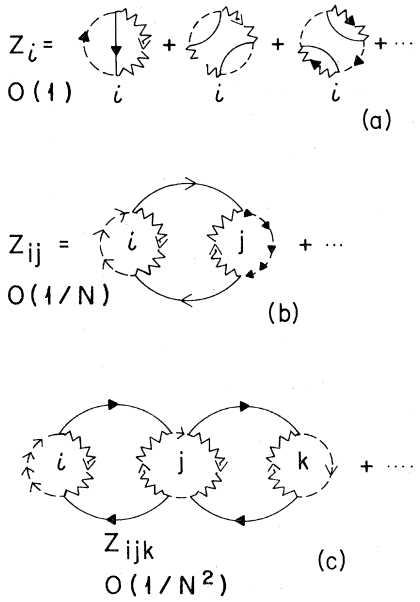

FIG. 10. Terms contributing to the cluster expansion of the mixed-valence lattice partition function. (a) Z_i, (b) Z_{ij}, and (c) Z_{ijk}, showing the dependence on N.

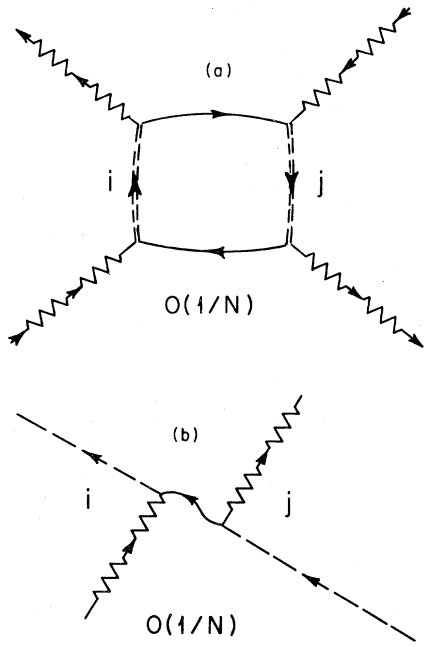

FIG. 11. Dominant $O(1/N)$ interaction terms in the mixed-valence lattice. (a) Interaction between empty states. (b) Hopping matrix element for f electrons.

IV. SUMMARY

This paper has shown how the introduction of zero-energy bosons to represent the singlet valence states of mixed-valence ions allows a simple reformulation of the mixed-valence problem that is far more amenable to conventional field-theory techniques. As an illustration of the application of this technique, a conventional Feynman-diagram expansion for mixed valence is developed: The applications of this expansion to the mixed-valence impurity have been presented in detail. The extension of this approach to the lattice has been discussed and outlined.

ACKNOWLEDGMENTS

The author thanks P. W. Anderson for his advice and encouragement during this work, and also T. V. Ramakrishnan who started the line of thought leading to this project. He thanks F. D. M. Haldane, C. M. Varma, and Hidenaga Yamagishi for their valuable discussions. This work was supported by a grant from the Science and Engineering Research Council, Swindon, Wiltshire, United Kingdom, for which the author is most grateful.

APPENDIX A: CALCULATION OF SELF-ENERGIES TO $O(1/N^2)$

The procedure for calculating a diagram is to explicitly evaluate a diagram at finite λ, then to take the large-λ limit. Figure 7 displays the diagrams for a $O(1/N^2)$ calculation of the self-energies $\Pi(\nu;\lambda)$ and $\Sigma_{fm}(\omega;\lambda)$. To evaluate the diagrams the full propagators $D(i\nu_n;\lambda)$ and $G_{fm}(i\omega_n;\lambda)$ are first expanded in terms of their spectral densities,

$$D(i\nu_n;\lambda)=\int_{-\infty}^{+\infty} d\omega (i\nu_n-\lambda-\omega)^{-1}B(\omega;\lambda)\ ,$$
$$G_{fm}(i\omega_n;\lambda)=\int_{-\infty}^{+\infty} d\nu (i\omega_n-\lambda-\nu)^{-1}A_{fm}(\nu;\lambda)\ . \tag{A1}$$

In terms of the propagators the algebraic expression of the diagrams is

$$\Pi(i\nu_n;\lambda)=(-1)\left[-k_BT\sum_{i\omega_n,\vec{k},m}|V(\vec{k})|^2 G_{km}(i\omega_n)\times G_{fm}(i\nu_n+i\omega_n;\lambda)\right], \tag{A2}$$
$$\Sigma_{fm}(i\omega_n;\lambda)=-k_BT\sum_{i\nu_n,\vec{k}}|V(\vec{k})|^2 G_{km}(i\omega_n-i\nu_n)\times D(i\nu_n;\lambda)\ ,$$

where the additional minus sign in the first equation is due to a closed fermion loop. The insertion of (A1) into (A2) and carrying out of the frequency summations leads to

$$\Pi(i\nu_n;\lambda)=\sum_{\vec{k},m}|V(\vec{k})|^2\int_{-\infty}^{+\infty} d\omega A_{fm}(\omega;\lambda)\times\frac{f(E(k))-f(\lambda+\omega)}{i\nu_n-\lambda+E(k)-\omega}\ , \tag{A3}$$
$$\Sigma_{fm}(i\omega_n;\lambda)=\sum_{\vec{k}}|V(\vec{k})|^2\int_{-\infty}^{+\infty} d\nu B(\nu;\lambda)\times\frac{1-f(E(k))-n(\lambda+\nu)}{i\omega_n-\lambda-E(k)-\nu}\ .$$

Here, $f(\omega)=(1+e^{\beta\omega})^{-1}$ is the Fermi function and $n(\omega)=(e^{\beta\omega}-1)^{-1}$ is the Bose function. In the limit $\lambda\to\infty$, the integrals over $f(\lambda+\omega)$ and $n(\lambda+\nu)$ vanish because the limiting spectral-weight functions $A_{fm}(\omega)$ and $B(\omega)$ have no weight at $\omega=-\lambda$ (see Appendix B). So omitting these terms and simplifying using formulas (A1) yields

$$\Pi(\nu)=\lim_{\lambda\to\infty}\Pi(\nu+\lambda;\lambda)=\sum_{\vec{k},m}|V(\vec{k})|^2 f(E(k))\times G_{fm}(\nu+E(k))\ , \tag{A4}$$
$$\Sigma_{fm}(\omega;\lambda)=\lim_{\lambda\to\infty}\Pi(\omega+\lambda;\lambda)=\sum_{\vec{k}}|V(\vec{k})|^2[1-f(E(k))]\times D(\omega-E(k))\ .$$

If the band and matrix elements are assumed to be symmetric about the Fermi surface the second equation attains the form used in (40).

APPENDIX B: SPECTRAL DECOMPOSITION OF BOSON AND FERMION PROPAGATORS

The full boson and fermion propagators of the grand-canonical ensemble may be spectrally decomposed as

$$G_{fm}(\tau;\lambda)=\langle T[f_m(\tau)f_m^\dagger(0)]\rangle_\lambda=\int_{-\infty}^{+\infty} d\omega\, e^{-(\omega+\lambda)\tau}[1-f(\omega+\lambda)]A_{fm}(\omega;\lambda)\ ,$$
$$D(\tau;\lambda)=\langle T[b(\tau)b^\dagger(0)]\rangle_\lambda=\int_{-\infty}^{+\infty} d\nu\, e^{-(\nu+\lambda)\tau}[1+n(\nu+\lambda)]B(\nu;\lambda)\ , \tag{B1}$$

where $\tau>0$ has been arbitrarily taken. By explicitly expanding the expectation values in terms of the eigenstates of the grand canonical ensemble $|i;Q_i\rangle$, $A_{fm}(\omega;\lambda)$, and $B(\nu;\lambda)$ can be explicitly written as

$$A_{fm}(\omega;\lambda)=\left[\sum_{i,j}|\langle j;Q_j|f_m^\dagger|i;Q_i\rangle|^2(e^{-\beta(E_j+\lambda Q_j)}+e^{-\beta(E_i+\lambda Q_i)})\delta(\omega-(E_j-E_i))\right]\Big/Z_G(\lambda)\ ,$$
$$B(\nu;\lambda)=\left[\sum_{i,j}|\langle j;Q_j|b^\dagger|i;Q_i\rangle|^2(e^{-\beta(E_j+\lambda Q_j)}+e^{-\beta(E_i+\lambda Q_i)})\delta(\nu-(E_j-E_i))\right]\Big/Z_G(\lambda)\ . \tag{B2}$$

Now taking the $\lambda\to\infty$ limit leads to

$$A_{fm}(\omega)=\left[\sum_{i,j}|\langle j;Q=1|f_m^\dagger|i;Q=0\rangle|^2 e^{-\beta E_i}\delta(\omega-(E_j-E_i))\right]\Big/Z_{\text{band}}\ ,$$
$$B(\nu)=\left[\sum_{i,j}|\langle j;Q=1|b^\dagger|i;Q=0\rangle|^2 e^{-\beta E_i}\delta(\nu-(E_j-E_i))\right]\Big/Z_{\text{band}}\ . \tag{B3}$$

In the $T\to0$ limit the dominant contribution to the sum over i in these expressions comes from the ground state of the $Q=0$ subspace $|0;Q=0\rangle$. This is merely the unperturbed sea of band electrons. Measuring energies relative to the energy of this state, then $Z_{\text{band}}\to1$ and the $T\to0$ limits of A and B are

$$A_{fm}^+(\omega)=\sum_i|\langle i;Q=1|f_m^\dagger|0;Q=0\rangle|^2\delta(\omega-E_i)\ ,$$
$$B^+(\nu)=\sum_i|\langle i;Q=1|b^\dagger|0;Q=0\rangle|^2\delta(\omega-E_i)\ . \tag{B4}$$

Here the E_i are the energies of the $Q=1$ eigenstates,

which all exceed E_0, the energy of the $Q=1$ ground state. Thus A^+ and B^+ are zero at frequencies below E_0.

Now from (B3),

$$A_{fm}(\omega)e^{-\beta\omega}=\left[\sum_{i,j}|\langle j;Q=1|f_m^\dagger|i;Q=0\rangle|^2 \times e^{-\beta E_j}\delta(\omega-(E_j-E_i))\right]\Big/Z_{\text{band}}\,,$$
$$B(\nu)e^{-\beta\nu}=\left[\sum_{i,j}|\langle j;Q=1|b^\dagger|i;Q=0\rangle|^2 \times e^{-\beta E_j}\delta(\nu-(E_j-E_i))\right]\Big/Z_{\text{band}}\,. \tag{B5}$$

In the zero-temperature limit, the sum over j are dominated by the ground state of the F_1 subspace, $|O;Q=1\rangle$. So normalizing these expressions by dividing by $Z_{\text{MV}}(\beta)$, they have zero-temperature limits given by

$$\begin{aligned}a_{fm}(\omega)&=\lim_{T\to 0}A_{fm}(\omega)e^{-\beta\omega}/Z_{\text{MV}}(\beta)\\&=\sum_i|\langle i;Q=0|f_m|0;Q=0\rangle|^2\delta(\omega-(E_0-E_i))\,,\\ b(\nu)&=\lim_{T\to 0}B(\nu)e^{-\beta\nu}/Z_{\text{MV}}(\beta)\\&=\sum_i|\langle i;Q=0|b|0;Q=1\rangle|^2\delta(\nu-(E_0-E_i))\,.\end{aligned} \tag{B6}$$

The $Q=1$ ground-state energy E_0 is less than the $Q=0$ ground-state energy because hybridization lowers the energy of the system, and thus $E_0<0$. The excited states of the $Q=0$ subspace have $E_i>0$, so that $E_0-E_i<0$, and also so that $a_{fm}(\omega)$ and $b(\nu)$ are zero for frequencies above E_0. Combining the results (B4) and (B6) leads to the results quoted in (42).

[1] C. M. Varma, Rev. Mod. Phys. 48, 219 (1976).
[2] *Valence Fluctuations in Solids*, edited by L. M. Falikov, W. Hanke, and B. Maple (North-Holland, Amsterdam, 1981).
[3] P. W. Anderson, Phys. Rev. 126, 41 (1961).
[4] J. Hubbard, Proc. R. Soc. London, Ser. A 277, 237 (1964).
[5] H. Keiter and J. C. Kimball, Int. J. Magn. 1, 233 (1971).
[6] A. Bringer and H. Lustfield, Z. Phys. B 28, 213 (1977).
[7] F. C. Zhang and T. K. Lee, Phys. Rev. B 28, 33 (1983).
[8] T. V. Ramakrishnan, Rev. Mod. Phys. 48, 13 (1976).
[9] N. Grewe and H. Keiter, Phys. Rev. B 24, 4420 (1980).
[10] K. W. H. Stevens, *Proceedings of the International Conference on Valence Fluctuations, Zurich, 1982* (North-Holland, Amsterdam, 1982).
[11] S. E. Barnes, J. Phys. F 6, 1375 (1976); 7, 2637 (1977).
[12] P. Coleman, Phys. Rev. B 28, 5255 (1983).
[13] J. M. Luttinger, Phys. Rev. 119, 1153 (1960).
[14] O. Gunnarson and K. Schonhammer, Phys. Rev. Lett. 50, 604 (1983).
[15] C. Itzykson and J. Zuber, *Quantum Field Theory* (McGraw-Hill, New York, 1980).
[16] F. D. M. Haldane, Phys. Rev. Lett. 40, 416 (1978).
[17] P. W. Anderson, Phys. Rev. Lett. 18, 1049 (1967).
[18] P. Nozieres and C. De Dominicis, Phys. Rev. 178, 1097 (1968).
[19] H. R. Krishnamurthy, J. W. Wilkins, and K. G. Wilson, Phys. Rev. B 21, 1044 (1980).
[20] N. Read and D. M. Newns, J. Phys. C 16, 3273 (1983).
[21] E. Witten, Nucl. Phys. B 145, 110 (1978).